Change of the surface electronic structure of Au(111) by a monolayer MgO(001) film

Yi Pan,[1] Stefania Benedetti,[2] Niklas Nilius,[1,*] and Hans-Joachim Freund[1]

[1]*Fritz-Haber-Institut der Max-Planck-Gesellschaft, Faradayweg 4-6, D-14195 Berlin, Germany*
[2]*CNR - Consiglio Nazionale delle Ricerche, Istituto Nanoscienze, Centro S3, Via G. Campi 213/a, 41100 Modena, Italy*

Monolayer films of MgO(001) have been prepared on an Au(111) surface and explored by means of scanning tunneling microscopy (STM) and spectroscopy. The symmetry mismatch between the hexagonal substrate and the squared overlayer results in the formation of a (6×1) superlattice, as revealed from the distinct stripe pattern observed in the STM images. The presence of the oxide film also modifies the potential situation at the interface, which induces a substantial upshift of the Shockley-type surface band on Au(111). The resulting MgO/Au interface band is characterized by a pseudogap at around 500 mV that opens at the position of the new Brillouin zone of the enlarged (6×1) unit cell. In addition the oxide layer gives rise to a drastic decrease of the Au(111) work function, as deduced from the energy position of the first field-emission resonance on the bare and MgO-covered surface. The work-function drop is explained by an interfacial charge transfer from the oxide film into the electro-negative gold surface.

I. INTRODUCTION

Thin oxide films on metal supports have an enormous technological impact and can be found in fields as diverse as optics, microelectronics, heterogeneous catalysis, and material sciences. Their applications range from corrosion protection,[1] antireflective coatings, insulating spacer-layers for magnetic[2,3] and electronic devices[4] to new materials with outstanding mechanical properties. Also the next generation of high-brightness photocathode materials might be based on thin-film technology, exploiting the substantial reduction of the metal work-function by an oxide layer.[5] Finally, oxide films turned out to be highly beneficial for promoting the catalytic activity of metal surfaces, as recently demonstrated for the CO oxidation on Pt-supported FeO films.[6]

The outstanding properties of thin-film systems rely on various aspects. The dielectric layer blocks the direct contact between the substrate and the surrounding gas-phase and keeps the metal surface in a defined state. It modifies the substrate electronic structure, e.g., by creating new electronic states at the interface or altering the energy position of existing ones.[7–9] And, it changes the work function of the metal by promoting charge-transfer processes that in turn lead to interfacial dipoles.[9,10] Naturally, electronic states with a high density-probability at the surface, such as surface and image-potential states, are most affected by the presence of a dielectric layer. The same holds for excitations with pronounced surface character, e.g., surface and interface plasmons.[11,12] Those surface-specific modes are consequently well suited to analyze the electronic interplay between a metal and a dielectric film.

The properties of thin-film systems have been widely investigated with electron and optical spectroscopy as well as with different theoretical approaches.[13–16] On the local scale, primarily the scanning tunneling microscope (STM) and its spectroscopic applications were used to study dielectric overlayers.[17] The probed material combinations ranged from oxide,[15,17,18] halide,[19,20] and semiconductor films[7] to layers of organic[21,22] and inorganic molecules[23–25] deposited on a variety of metal supports. Shifts of image-potential and surface states stood in the focus of the experiments, as they provide insight into the work function and potential course at the interface.

This paper reports on how a single layer of MgO(001) affects the electronic properties of the Au(111) surface. We have chosen this particular metal/oxide combination for two reasons. The substrate exhibits a Shockley-type surface state and therewith a well-characterized electronic fingerprint.[26,27] MgO, on the other hand, is a typical ionic insulator, which interacts with the Au surface mainly via polarization forces and not via interfacial bond-formation. Already several substrates have been used to grow MgO layers, including Ag(001),[28–30] Fe(001),[3] and Mo(001);[31] however, none of them exhibit a surface state. Furthermore, the symmetry mismatch between the hexagonal gold and the square MgO(001) leads to unusual electronic effects, such as the development of a new Brillouin zone and the associated opening of electronic gaps.[32] Both phenomena render MgO on Au(111) an interesting model system to gain a better understanding of metal/oxide interfaces.

II. EXPERIMENT

The experiments have been performed in an ultrahigh-vacuum STM operated at 4.5 K. Electronic properties of the system were derived from differential conductance (dI/dV) spectra measured with lock-in technique. The MgO films are prepared by depositing ∼0.5-ML Mg in an oxygen ambience onto a sputtered/annealed Au(111) surface held at elevated temperature. Two distinct growth modes can be distinguished. At low temperature and O_2-partial pressure (500 K, 1×10^{-7} mbar), triangular MgO(111) patches with a hexagonal diffraction pattern develop, while MgO(001) islands with a square symmetry form at a higher temperature and in an excess of oxygen (650 K, 5×10^{-6} mbar, Fig. 1). In both regimes a small part of the MgO does not fully crystallize, but forms three-dimensional (3D) islands with irregular shapes. In this paper we concentrate on the square MgO(001) phase, while the polar MgO(111) will be discussed in a separate publication.[33]
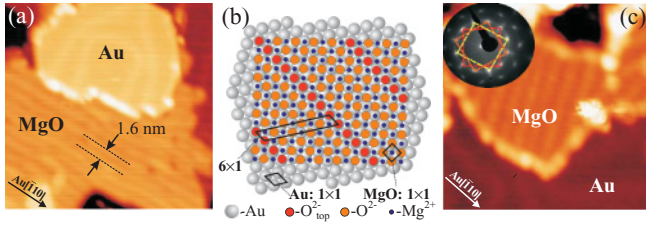
FIG. 1. (Color online) STM topographic images of MgO(001) islands on Au(111) (a) 30 × 30 nm², 1.0 V and (c) 20 × 20 nm², 2.5 V. (b) Structure model of the monolayer oxide-film with the respective unit cells indicated. The inset shows a LEED pattern of the MgO/Au(111) system, displaying the three rotational oxide domains.

III. RESULTS AND DISCUSSION

The MgO(001) patches are readily identified in the STM topographic images thanks to their distinct parallel-stripe pattern that differs from the zig-zag lines of the herringbone reconstruction on bare Au(111) (Fig. 1). The islands are often surrounded by a narrow brim of irregular MgO clusters. The stripe pattern occurs in three rotational domains running along equivalent Au⟨$\bar{1}$10⟩ directions and has a line spacing of (1.6 ± 0.1) nm. It can be assigned to a coincidence lattice formed between the hexagonal Au(111) ($d_{Au-Au} = 0.289$ nm) and the square MgO(001) unit cell ($d_{O-O} = 0.297$ nm) [Fig. 1(b)] with the MgO[110] vector running parallel to an Au⟨$\bar{1}$10⟩ direction. Along this direction the oxide is in registry with the support, which requires a 3% compression of the bulk MgO-lattice parameter. In the perpendicular direction only row matching is feasible because of the deviating lattice symmetry. Here, five Mg-O double rows overgrow six Au rows ($d_{row-row} = 0.25$ nm), resulting in a (6 × 1) superstructure. In each coincident cell, one O and one Mg atom bind directly on top of an Au atom, while all other atoms sit in various bridge and hollow sites. The associated modulation in the interface geometry produces the stripe pattern in the STM. The fact that the pattern is visible best at positive bias and becomes faint at negative polarity suggests a certain electronic contribution to the contrast (Fig. 2).
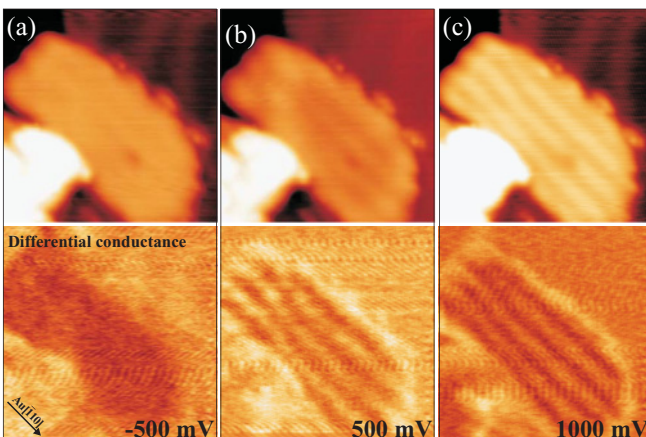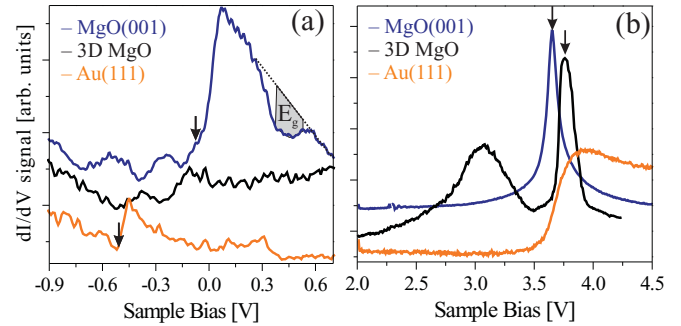

FIG. 3. (Color online) Differential conductance spectra of bare Au(111), the MgO monolayer, and a 3D-MgO cluster taken (a) around the Fermi level and (b) at elevated positive bias. Whereas the onsets of the Au(111) surface and MgO/Au(111) interface band are detected in (a) (see arrows), the *L*-edge in Au(111), the conduction band onset in the 3D MgO and the first FERs (see arrows) are observed in (b).

The electronic structure of the monolayer MgO(001) is probed with *dI/dV* spectroscopy and imaging performed in a broad bias-window. On bare Au(111), the step-like onset of the Shockley surface-band at −500 mV dominates the low-bias *dI/dV* spectra [Fig. 3(a)].[27] On the MgO(001) islands, this spectral feature is replaced by a much higher step at −90 mV, which governs the *dI/dV* response up to +700 mV sample bias. The 3D-MgO clusters, on the other hand, do not display any discernable structure in this bias range, indicating the full development of the oxide band-gap. The Shockley surface-state on Au(111) comes along with a characteristic wave pattern that can be observed in STM-conductance images taken around the Fermi level (E_F, Fig. 4). The pattern reflects charge-density oscillations that result from the interference of surface waves impinging and recoiling from the gold step-edges. Its periodicity depends on the inverse wave vector of the surface-state electrons, $\lambda_{dI/dV} = \pi/k$ and changes with sample bias. The wave vector extracted from *dI/dV* images can thus be used to determine the dispersion relation of the Au(111)-surface electrons, although the STM is not intrinsically *k*-sensitive. A respective analysis reveals the

FIG. 2. (Color online) (a)-(c) Topographic (upper row) and *dI/dV* images (lower row) of MgO(001) islands on Au(111) taken at the indicated bias voltage (16 × 16 nm²).
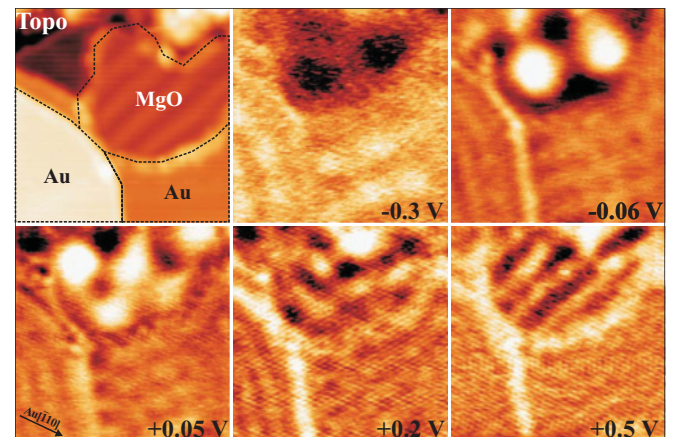

FIG. 4. (Color online) Topographic and *dI/dV* images of two Au(111) terraces and a monolayer MgO(001) island taken at the indicated bias voltage (15 × 15 nm²).
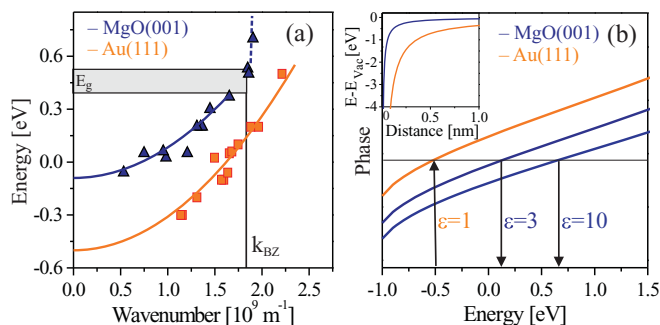
FIG. 5. (Color online) (a) Dispersion of the Au(111) surface and MgO/Au(111) interface band, as deduced from conductance images similar to the ones shown in Fig. 4. The lines are parabolic functions fitted to the data. The new Brillouin zone of the MgO/Au(111) (6 × 1) cell and the resulting band gap are indicated. No dispersion is detected beyond this gap position. (b) Energy-dependent scattering phase for the vacuum/Au(111) and MgO/Au(111) interfaces, calculated with the phase-accumulation model. The oxide film is described by two different dielectric constants. The inset displays the image-potential course at the two interfaces.

expected parabolic *E-k* dependency, being described by an onset-energy of −500 meV and an effective electron mass of $0.22m_e$ [Fig. 5(a)]. Both parameters match the results of earlier STM and photoelectron-spectroscopy measurements performed on Au(111) single crystals.[26,27]

A similar wave pattern is observed also in regions that are covered with the monolayer MgO film (Fig. 4). In contrast to bare Au(111) it emerges at bias voltages close to zero when localized maxima develop in the *dI/dV* images, and transforms into the characteristic line pattern only at higher bias. The line spacing gradually decreases with bias until it reaches a constant value of 1.6 nm at 0.5 V. At higher bias, the *dI/dV* images perfectly follow the stripe pattern visible in the STM topographies, which were assigned to the coincidence lattice before (Fig. 2). Again, the *E-k* dependence is reconstructed from the bias-dependent conductance behavior of the MgO islands, yielding an onset-energy of −90 mV and an effective electron mass of $0.20m_e$ [Fig. 5(a)]. A comparison with the dispersion relation obtained for Au(111) reveals a similar slope, but a characteristic energy shift of the two curves. It should be noted that the bias window in which the wave patterns appear on MgO(001) coincides with the *dI/dV* step in the spectroscopy data, suggesting a similar origin.

The second spectral region of interest is the one of the field-emission resonances (FERs), which starts above the sample work-function [Fig. 3(b)]. FERs are vacuumlike states that develop in the classical part of the tip-sample cavity and dominate the electron transport between tip and sample at higher bias.[34] While higher FERs depend strongly on the tip-electric field, the lowest mode relates to the image potential states and provides a rough measure of the sample work function. FER spectroscopy has been performed with enabled feedback loop in order to increase the dynamic range of the measurements. On bare gold a pronounced *dI/dV* step at 3.5 V is revealed that indicates the upper edge of the Au *L*-gap.[26] The first FER appears at 5.25 V on Au(111) but shifts to 3.6 and 3.8 V for the monolayer and 3D-oxide islands,

respectively [Fig. 3(b)]. A second peak in the spectrum of the MgO cluster marks the conduction-band onset at 2.9 V. The feature is not detected for the (001) film, although the band gap should be developed also in the monolayer limit, as shown for MgO/Ag(001).[20] We relate the missing spectral signature to the smallness of the *dI/dV* change induced by the band onset.

The spectral information contained in the two energy windows discussed above provides insight into the electronic structure at the MgO(001)/Au(111) interface. The most pronounced low-bias effect is the transformation of the Au(111)-surface band into a gold-dominated interface band and the associated shift of the band onset from −500 to −90 mV. In a qualitative picture the shift arises from the faster decline of the image potential outside the Au surface because of the high dielectric constant of the oxide film.[25,35] This leaves less space for the development of the surface state, pushing it to higher energies where the potential well becomes more spacious [Fig. 5(b), inset]. A quantitative approximation of the shift can be obtained from the phase-accumulation model developed by N. V. Smith.[36] Here, the energy of the surface state is given by a Sommerfeld-type quantization condition, in which the phase of a scattered electron at the crystal- and surface-side of the interface accumulates to zero: $\phi_c + \phi_s = 0$. The surface phase is derived from the classical image potential modified by the dielectric constant $\varepsilon_{MgO} = 10$, and the work function change $\Delta\Phi$ induced by the dielectric layer $\phi_s(E) = \sqrt{\frac{3.4eV/\varepsilon_{MgO}^2}{E_{vac} - \Delta\Phi - E}} - \pi$. Whereas $\Delta\Phi$ is estimated from the shift of the first FER when going from the bare to the oxide-covered surface (see subsequent discussion), the Au(111)-vacuum energy is set to its literature value of $E_{vac} = 5.3$ eV.[25] The crystal phase, on the other hand, is determined from the position of the upper $(E_{up} = 3.5$ eV) and lower edge $(E_{low} = -1.0$ eV) of the *L*-gap in Au(111): $\phi_c(E) = 2 \arcsin\sqrt{\frac{E - E_{low}}{E_{up} - E_{low}}}$. The sum of both phases as a function of energy is plotted in Fig. 5(b) for the bare and MgO-covered surface. To account for contributions that are not included in the phase-accumulation model, the critical phase at which the surface state occurs is determined from the known position of the Au(111)-surface state.[36] The same phase is reached at +580 meV for the MgO(001)/Au(111) interface, reflecting the upshift of the interface band as seen in the experiment. However, the calculated shift is much larger than the measured one, which indicates the limits of the phase-accumulation model. Similar deviations were found before for interface states between Au(111) and different rare-gas layers,[25] while a better agreement was claimed for the NaCl/Cu(111) system.[19] The most relevant simplification in the model is the assumption of an infinitely thick MgO film to calculate the image-potential course. In reality the potential declines quickly only within a single-oxide layer, while beyond the dielectric response is governed by vacuum again. Including this effect leads to a widening of the upper part of the potential well and a downshift of the MgO/Au interface state. Furthermore, the dielectric constant of a thin MgO layer certainly differs from the bulk behavior assumed here. Experiments on ultrathin oxide films always found a reduction of the dielectric constant, being explained by the finite number of polarizable units.[37,38] Indeed a decrease of ε_{MgO} to three leads to a better match between the measured and

the calculated onset of the MgO/Au interface state, although the crudeness of the model does not allow for any quantitative conclusions.

Apart from potential changes perpendicular to the surface, the MgO(001) layer also introduces a new periodicity within the plane. As discussed, the simple (1×1) cell of Au(111) transforms into a (6×1) cell in the MgO/Au ad-system. This structural modification gives rise to a new zone boundary in reciprocal space, being located at 1/6 of the original value in the direction perpendicular to the stripe pattern. The new quasi-1D Brillouin zone becomes manifest in the dI/dV spectra of the metal/oxide system. It sets the maximum wave vector for electrons propagating perpendicular to the stripes to $k_{BZ} = \pi/6d_{Au-Au} = 1.8 \times 10^9$ nm^{-1} and hence the minimum real-space distance between the wavecrests to 1.7 nm. Indeed, no change in the periodicity of the stripe pattern is observed anymore once this critical distance is reached (Fig. 2). In addition a partial band gap opens at the new zone boundary. Its size is estimated to (120 ± 20) meV, giving a measure for the perturbation potential introduced by the oxide layer.[19] The midgap position can be determined from the respective k_{BZ} value in the dispersion relation to be around 450 mV [Fig. 5(a)]. In fact a clear dip appears in dI/dV spectra of the oxide film at the predicted bias position [Fig. 3(a)]. The conductance signal in the gap remains finite because the new zone boundary occurs only in the direction perpendicular to the stripes. Finally, we want to comment on the surprisingly large intensity of MgO/Au interface states in dI/dV spectroscopy.[22,35] The modified Shockley band provides most of the states for electron tunneling into/out of the MgO islands because of the oxide band-gap, but competes with a high density of bulklike states on pristine Au(111). In addition the spatial extension of the surface states into the vacuum might be altered by the dielectric layer, giving rise to a better overlap with the tip wave-functions.

The high-bias dI/dV spectra of MgO/Au(111) can be interpreted in terms of a work-function change induced by the oxide film. Based on the position of the first FER on bare Au (5.2 V) and MgO ad-islands (3.6 V), the shift is determined with -1.6 V. This reduction occurs already for a single MgO layer and changes only weakly with film thickness, as expected for an interface effect. The size of $\Delta\Phi$ results from the competition of three interface dipoles. The first one is induced by the charge transfer from the MgO into the electronegative Au. The second one describes the polaronic response of the oxide film, and leads to an outward relaxation of the O^{2-} with respect to the Mg^{2+}. And the final one originates from the suppression of electron spill-out at the Au surface. While the first two contributions almost cancel each other, the last one gives rise to a net reduction of the work function.[9,10] The work-function change has been analyzed for various metal/oxide systems, including MgO/Ag(001), MgO/Pd(001), and MgO/Mo(001). In the latter cases $\Delta\Phi$ was found to scale with the electronegativity of the substrate, a trend that is now confirmed for Au(111).[9] Gold is the most electronegative of all the considered metals and consequently exhibits the largest work function drop upon MgO deposition: $(\Delta\phi_{Au} = -1.6$ eV, $\Delta\phi_{Mo} = -1.5$ eV, $\Delta\phi_{Ag} = -1.0$ eV).[9,10,39] The MgO/Au(111) system might therefore be particularly suited to trigger charge transfer processes into adsorbates bound to the thin-film surface.

IV. CONCLUSION

The growth of monolayer MgO(001) islands has a pronounced effect on the surface electronic structure of the Au(111) support. It transforms the Shockley surface-state of gold into an interface band at considerably higher energy. This shift reflects the altered potential situation at the metal/oxide interface, in particular the fast decline of the image potential attributable to the high dielectric constant of MgO. A new Brillouin zone is introduced in reciprocal space as a result of the larger MgO/Au(111) unit cell. At the zone boundary a pseudogap opens in the interface band, giving rise to a dip in differential-conductance spectra around 450 mV. Furthermore, the MgO overlayer produces a strong interface dipole that results from charge-transfer processes across the interface. All those effects are already developed for monolayer-thick films, indicating the importance of interfacial interactions in metal/oxide systems. Our results demonstrate a possible route to modify the surface-electronic structure of a metal by depositing a suitable dielectric film on top.

ACKNOWLEDGMENTS

*Corresponding author: nilius@fhi-berlin.mpg.de

[1] D. A. Jones, *Principles and Prevention of Corrosion* (Prentice Hall, Upper Saddle River, 1995).

[2] C. Li and A. J. Freeman, Phys. Rev. B **43**, 780 (1991).

[3] H. L. Meyerheim, R. Popescu, J. Kirschner, N. Jedrecy, M. Sauvage-Simkin, B. Heinrich, and R. Pinchaux, Phys. Rev. Lett. **87**, 076102 (2001).

[4] J. Robertson, Rep. Prog. Phys. **69**, 327 (2006).

[5] K. Nemeth, K. C. Harkay, M. van Veenendaal, L. Spentzouris, M. White, K. Attenkofer, and G. Srajer, Phys. Rev. Lett. **104**, 046801 (2010).

[6] Y.-N. Sun, Z.-H. Qin, M. Lewandowski, S. Kaya, S. Shaikhutdinov, and H.-J. Freund, Catal. Lett. **126**, 12631 (2008).

[7] W. Mönch, Surf. Sci. **299**, 928 (1994); J. Vac. Sci. Technol. B **17**, 1867 (1999).

[8] G. Bordier and C. Noguera, Phys. Rev. B **44**, 6361 (1991).

[9] J. Goniakowski and C. Noguera, Interface Sci. **12**, 93 (2004); Phys. Rev. B **79**, 155433 (2009).

[10] G. Pacchioni, L. Giordano, and M. Baistrocchi, Phys. Rev. Lett. **94**, 226104 (2005); L. Giordano, F. Cinquini, and G. Pacchioni, Phys. Rev. B **73**, 045414 (2006).

[11] N. J. Halas, MRS Bull. **30**, 362 (2005).

[12] K. Welford, Opt. Quant. Electron **23**, 1 (1991).

[13] S. A. Chambers, Surf. Sci. Rep. **39**, 105 (2000).

[14] C. B. Harris, N. H. Ge, R. L. Lingle, J. D. McNeill, and C. M. Wong, Annu. Rev. Phys. Chem. **48**, 711 (1997).

[15] H.-J. Freund and G. Pacchioni, Chem. Soc. Rev. **37**, 2224 (2008).

[16] J. Gudde and U. Hofer, Prog. Surf. Sci. **80**, 49 (2005).

[17] N. Nilius, Surf. Sci. Rep. **64**, 595 (2009).

[18] S. C. Street, C. Xu, and D. W. Goodman, Ann. Rev. Phys. Chem. **48**, 43 (1997).

[19] J. Repp, G. Meyer, and K.-H. Rieder, Phys. Rev. Lett. **92**, 036803 (2004).

[20] M. Pivetta, F. Patthey, M. Stengel, A. Baldereschi, and W. D. Schneider, Phys. Rev. B **72**, 115404 (2005).

[21] D. Velic, A. Hotzel, M. Wolf, and G. Ertl, J. Phys. Chem. **109**, 9155 (1998).

[22] K. Andrews and T. P. Pearl, J. Chem. Phys. **132**, 214701 (2010).

[23] E. Bertel, Appl. Phys. A **53**, 356 (1991).

[24] D. C. Marinica, C. Ramseyer, A. G. Borisov, D. Teillet-Billy, J. P. Gauyacq, W. Berthold, P. Feulner, and U. Hofer, Phys. Rev. Lett. **89**, 046802 (2002).

[25] T. Andreev, I. Barke, and H. Hövel, Phys. Rev. B **70**, 205426 (2004).

[26] S. LaShell, B. A. McDougall, and E. Jensen, Phys. Rev. Lett. **77**, 3419 (1996).

[27] Y. Hasegawa and Ph. Avouris, Phys. Rev. Lett. **71**, 1071 (1993).

[28] J. Wollschläger, D. Erdos, H. Goldbach, R. Hopken, and K. M. Schröder, Thin Sol. Films **400**, 1 (2001).

[29] O. Robach, G. Renaud, and A. Barbier, Phys. Rev. B **60**, 5858 (1999).

[30] S. Schintke, S. Messerli, M. Pivetta, F. Patthey, L. Libioulle, M. Stengel, A. De Vita, and W. D. Schneider, Phys. Rev. Lett. **87**, 276801 (2001).

[31] S. Benedetti, H. M. Benia, N. Nilius, S. Valeri, and H.-J. Freund, Chem. Phys. Lett. **430**, 330 (2006).

[32] C. Hagendorf, R. Shantyr, H. Neddermeyer, and W. Widdra, Phys. Chem. Chem. Phys. **8**, 1575 (2006); C. Hagendorf, S. Sachert, B. Bochmann, K. Kostov, and W. Widdra, Phys. Rev. B **77**, 075406 (2008).

[33] S. Benedetti and N. Nilius (in preparation).

[34] G. Binnig, K. H. Frank, H. Fuchs, N. Garcia, B. Reihl, H. Rohrer, F. Salvan, and A. R. Williams, Phys. Rev. Lett. **55**, 991 (1985).

[35] H. Hövel, B. Grimm, and B. Rheil, Surf. Sci. **477**, 4 (2001).

[36] N. V. Smith, Phys. Rev. B **32**, 3549 (1985).

[37] S. W. Wu, G. V. Nazin, X. Chen, X.H. Qiu, and W. Ho, Phys. Rev. Lett. **93**, 236802 (2004).

[38] H. C. Ploigt, C. Brun, M. Pivetta, F. Patthey, and W. D. Schneider, Phys. Rev. B **76**, 195404 (2007).

[39] T. König, G. H. Simon, H.-P. Rust, and M. Heyde, J. Phys. Chem. C **113**, 11301 (2009).